Webb, A.A.G., Guo, H., Clift, P.D., Husson, L., Müller, T., Costantino, D., Yin, A., Xu, Z., Cao, H., and Wang, Q., 2017, The Himalaya in 3D: Slab dynamics controlled mountain building and monsoon intensification: Lithosphere, doi:10.1130/L636.1.

Data Repository Files for Webb et al., The Himalaya in 3D.

Figure DR1.

Over three pages following this explanatory text, this figure displays the compiled detrital thermochronology data shown in Figure 4 in two ways meant to permit more detailed interrogation. References and locations for each sample are listed in Table DR4.

On the second and third pages following this explanatory text, the compiled detrital thermochronology results from the Himalayan foreland basin are shown with data for each sample plotted in isolation. Here, red curves are fission track zircon data, and blue curves are $^{40}Ar/^{39}Ar$ muscovite data. The vertical lines indicate the depositional age, which is also listed along with the sample name and n number (the number of dates analysed and represented in the KDE plot).

On the first page following this explanatory text, the data is displayed in batches as in Figure 4C. That is, the plots distinguish by type (muscovite vs. zircon) and by depositional age in five million year age bins. In most plots, the highest probability peak for each sample is highlighted. These peaks are not highlighted in the $^{40}Ar/^{39}Ar$ muscovite plot for the 10 Ma to 5 Ma depositional age range because so many peaks are clustered between 19 Ma and 16 Ma that thickening the lines there would render the plot unreadable. Here, we describe the data as represented in these batch plots and discuss corresponding interpretations (particularly in comparison to the model presented in Figure 6):

$^{40}Ar/^{39}Ar$ muscovite:

Observations

- 25-20 Ma depositional age range: Three central Himalayan samples have Oligocene probability peaks.
- 20-15 Ma: One western Himalayan sample has a main probability peak at ~17.5 Ma, two have peaks at ~20.5 Ma, and the rest of the main peaks are Oligocene in age range. Central Himalayan peaks range from the Oligocene to a youngest peak at ~21 Ma.
- 15-10 Ma: Western Himalayan samples have main probability peaks ranging from ~26 Ma to ~18.5 Ma, whereas central Himalayan samples have a broader range of peaks from ~29 Ma to ~16.5 Ma.

- 10-5 Ma: Western Himalayan Himalayan foreland samples have probability peaks clustered at 19-18 Ma, whereas central Himalayan samples have peaks at 18-15 Ma. Each regional group has one sample dominated by older (generally Paleogene) dates.
- 5-0 Ma: A sample from the western Himalayan foreland is dominated by a major probability peak at just over 20 Ma, whereas three samples from the central Himalayan foreland are dominated by peaks at ~17 Ma (with one showing a sub-peak at ~15 Ma).

Interpretations

The range of $^{40}Ar/^{39}Ar$ muscovite main probability peak ages for Himalayan foreland samples narrows through time, such that results from samples with young depositional ages are dominated by ~21-15 Ma probability peaks. This pattern suggests relatively moderate cooling and exhumation rates prior to this period, rapid rates during this period, and low rates afterwards. Among samples recording dominant cooling in this ~21-15 Ma period, the main probability peaks for western Himalayan samples generally skew older than central Himalayan cooling peaks by 1 to 6 million years. For example, the youngest main cooling peak for a western Himalayan sample is ~17.5 Ma, whereas the youngest main cooling peak for a central Himalayan sample is ~15 Ma. This suggests that the rapid cooling and exhumation in the western Himalaya is older than that of the central Himalaya by three to four million years. The specific early to middle Miocene age peaks for both regions correspond well to South Tibet fault cessation timing in these regions (see Figures 2, 3), supporting the link of these processes discussed in the main text.

Fission track zircon:

Observations

- 15-10 Ma depositional age range: Four western Himalayan samples have main probability peaks from ~21.5 Ma to ~17.5 Ma, with the remaining two samples showing Paleogene main peaks. One central Himalayan main peak is ~11 Ma, and three others are tightly clustered between ~17.5 Ma and ~17 Ma. Two east-central Himalaya samples have main peaks at ~14 Ma and ~12 Ma.
- 10-5 Ma: Central Himalayan samples have main probability peaks from ~17 Ma to ~10 Ma; east-central Himalayan samples have main probability peaks from ~10 Ma to ~7.5 Ma.

- 5-0 Ma: Central Himalayan samples have main probability peaks from ~12 Ma to ~5.5 Ma; east-central Himalayan samples have main probability peaks from ~8 Ma to ~5 Ma.

Interpretations

Fission track zircon thermochronology has a lower closure temperature versus $^{40}Ar/^{39}Ar$ muscovite, so detrital age populations are generally younger and there is less lag time between recorded cooling events and deposition. As discussed in the main text, the 15-10 Ma depositional time batch of detrital fission track zircon results shows a trend of decreasing age from the west to the east-central Himalaya which is broadly consistent with South Tibet fault cessation timing. The one exception is a central Himalayan sample with a young (~11 Ma) main age peak. In the interpretative framework provided in the main text, this sample may perhaps reflect a relatively local geological feature such as rapid footwall uplift along an east-west extending system developed in the wake of slab detachment. The younger depositional time batches also skew younger in the east-central Himalaya versus the central Himalaya. Main age probability peaks for the 10-5 Ma depositional batch may largely reflect cooling in response to slab detachment, as most east-central Himalayan samples have main peaks at ~10 Ma and the central Himalayan samples have main peaks up to ~17 Ma. Samples with younger depositional ages record cooling and exhumation after the main proposed slab detachment period.

Webb, A.A.G., Guo, H., Clift, P.D., Husson, L., Müller, T., Costantino, D., Yin, A., Xu, Z., Cao, H., and Wang, Q., 2017, The Himalaya in 3D: Slab dynamics controlled mountain building and monsoon intensification: Lithosphere, doi:10.1130/L636.1.

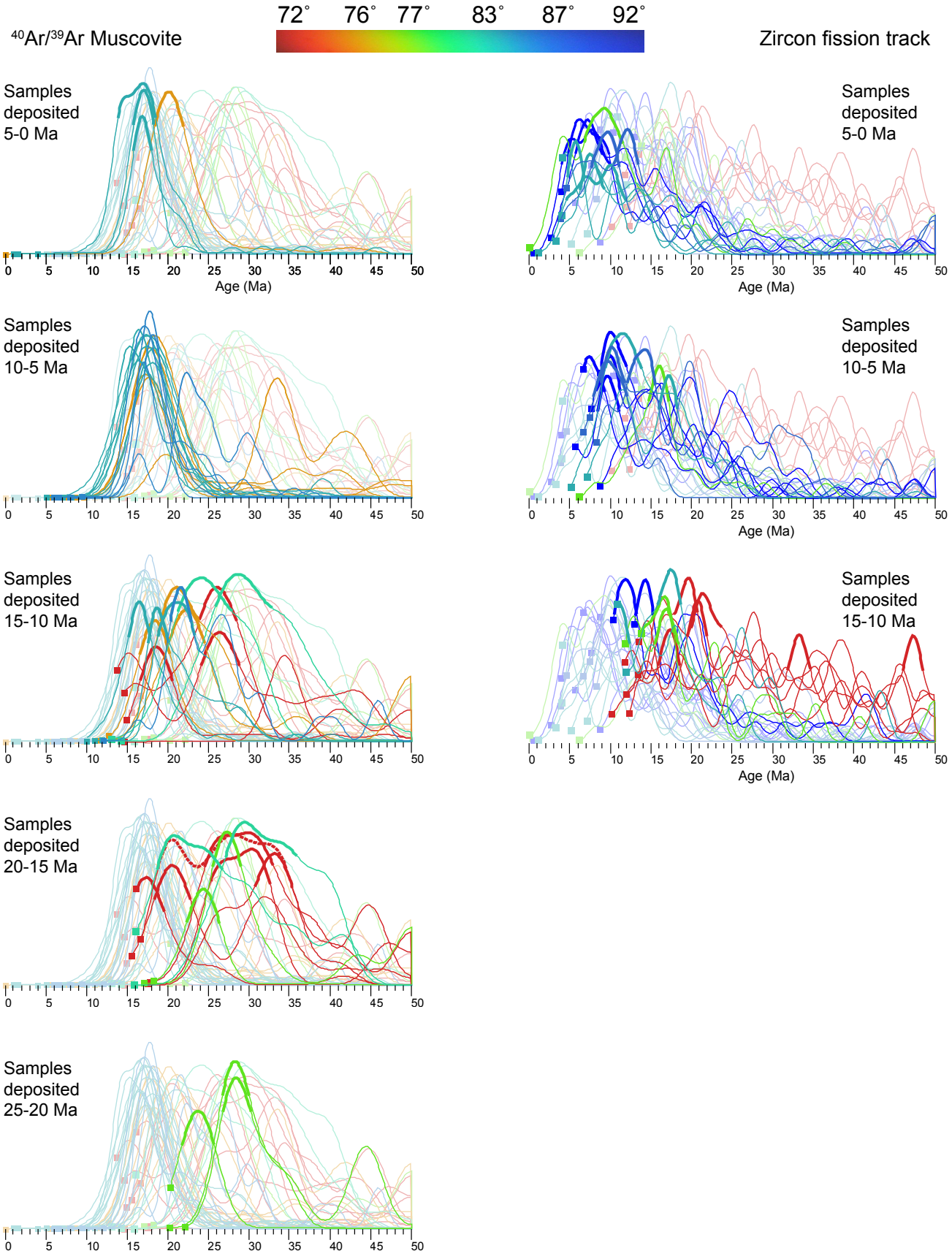

Figure DR1, Webb et al.

Webb, A.A.G., Guo, H., Clift, P.D., Husson, L., Müller, T., Costantino, D., Yin, A., Xu, Z., Cao, H., and Wang, Q., 2017, The Himalaya in 3D: Slab dynamics controlled mountain building and monsoon intensification: Lithosphere, doi:10.1130/L636.1.

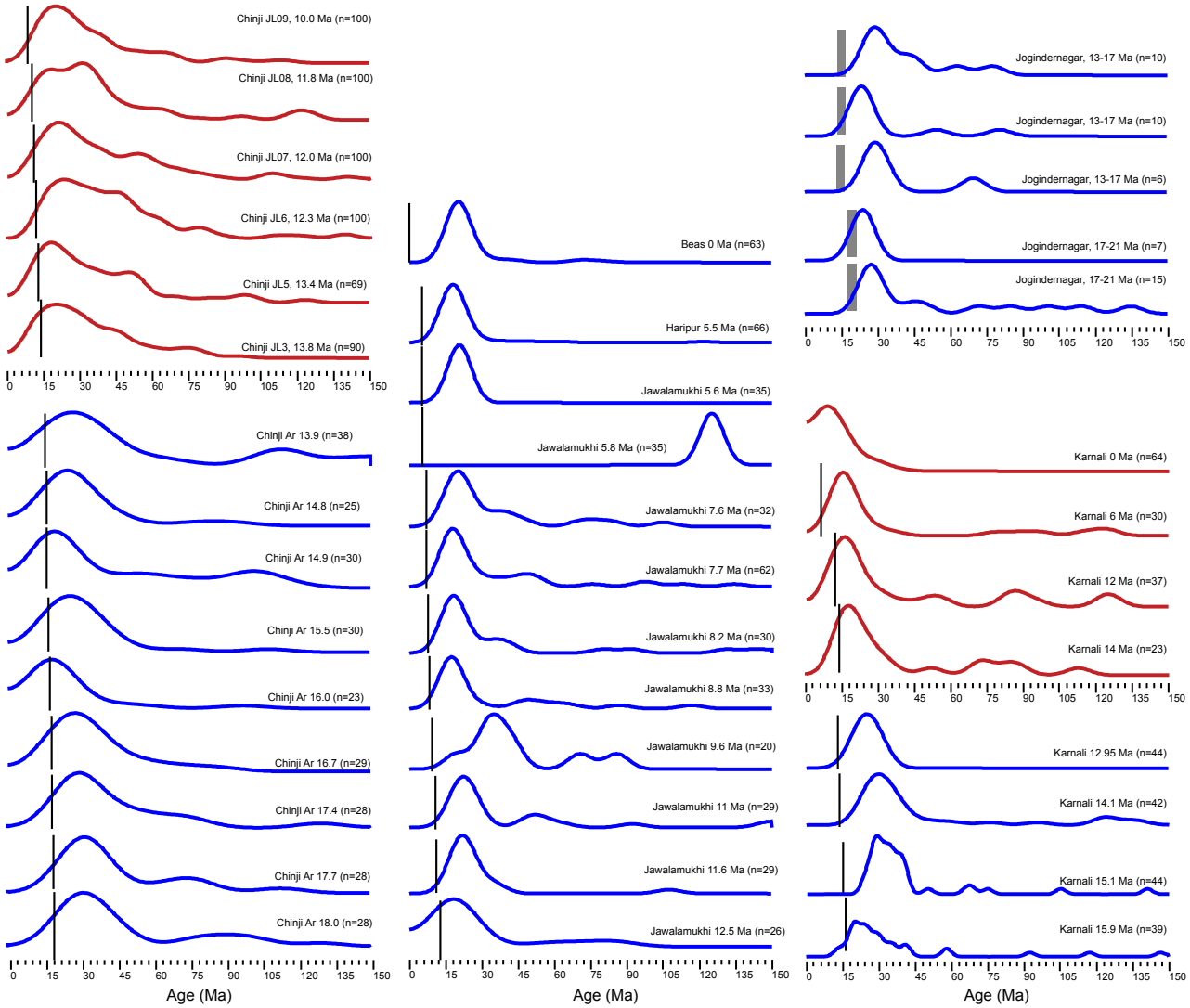

Figure DR1, continued, Webb et al.

Webb, A.A.G., Guo, H., Clift, P.D., Husson, L., Müller, T., Costantino, D., Yin, A., Xu, Z., Cao, H., and Wang, Q., 2017, The Himalaya in 3D: Slab dynamics controlled mountain building and monsoon intensification: Lithosphere, doi:10.1130/L636.1.

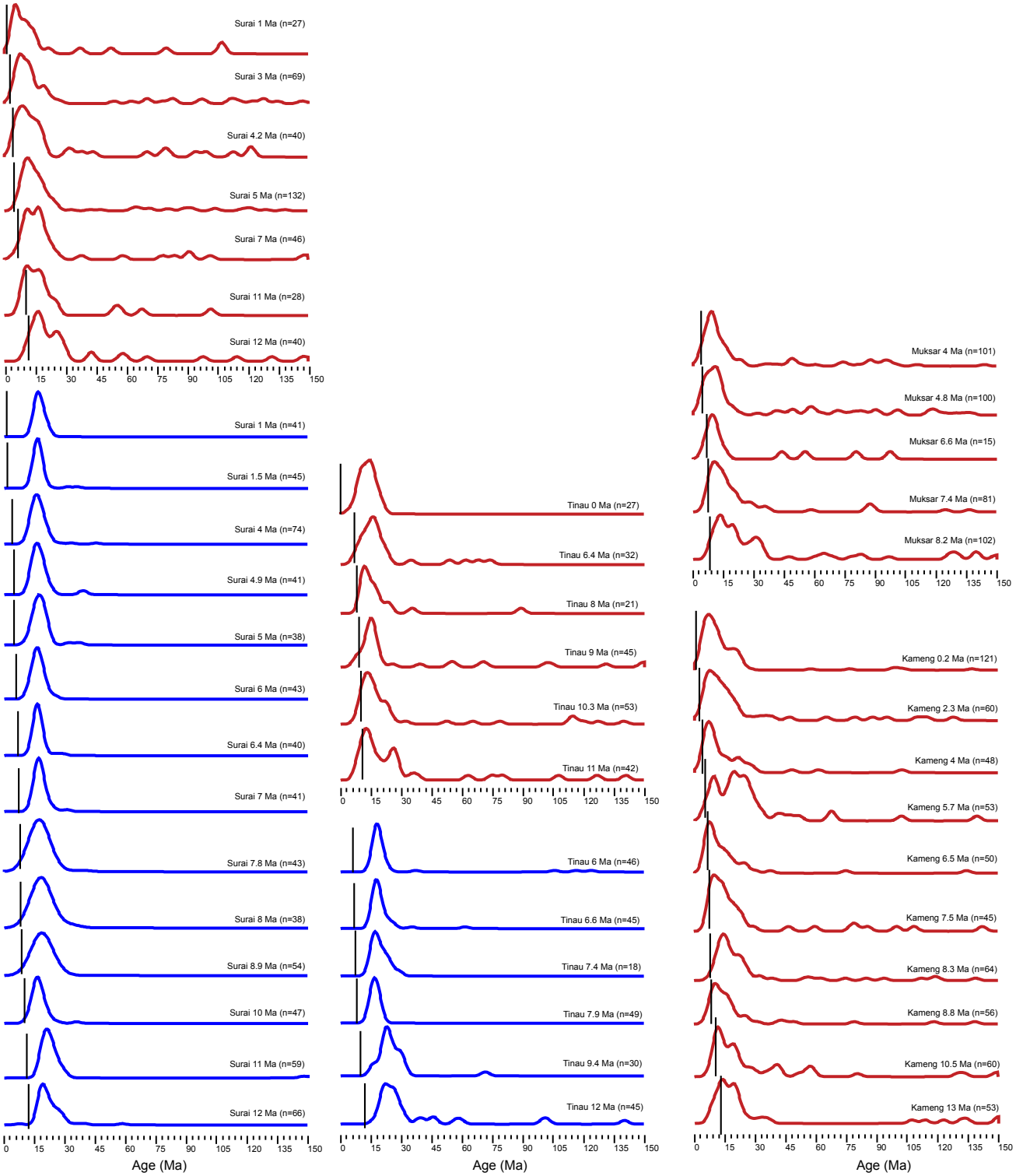

Figure DR1, continued, Webb et al.

Data Repository Tables.

Table DR1. Constraints on timing of cessation of South Tibet fault activity. These data are plotted in Figures 2 and 3. Details of the interpretation of fault motion cessation are discussed in the main text.

Latitude (°N)	Longitude (°E)	Region	Timing (Ma)	Basis	Source
34.0	76.0	NW Zanksar	>23.1--17.8	Footwall and shear zone $^{40}Ar/^{39}Ar$ muscovite ages	(Vance et al., 1998)
33.0	77.2	SE Zanskar	<22.1 ± 0.4	Mean of Th/Pb ages of igneous monazite in deformed leucogranite	(Horton et al., 2015)
33.0	77.2	SE Zanskar	>22--21	Mean of Th/Pb ages of igneous monazite and uraninite in undeformed leucogranite	(Horton et al., 2015; Walker et al., 1999)
33.0	77.2	SE Zanskar	>22.1--19.3	Footwall and shear zone base $^{40}Ar/^{39}Ar$ muscovite ages	(Dézes et al., 1999; Horton et al., 2015; Walker et al., 1999)
32.3	77.2	Beas	>22.2--20.6	Footwall, shear zone, and immediate hanging wall $^{40}Ar/^{39}Ar$ muscovite ages	(Schlup et al., 2011; Stübner et al., 2014; Walker et al., 1999)
31.7	78.0	Wanger	>18.6--15.5	Footwall, shear zone, and immediate hanging wall $^{40}Ar/^{39}Ar$ muscovite ages	(Thiede et al., 2005; Vannay et al., 2004)
31.6	78.3	Sutlej	>19.2--15.5	Footwall and hanging wall $^{40}Ar/^{39}Ar$ muscovite ages	(Vannay et al., 2004)
31.0	79.0	Gangotri	<23.0 ± 0.4	Mean U/Pb age of monazite in deformed leucogranite	(Searle et al., 1999)
30.7	79.9	Malari	>18.9 ± 0.6	Mean of U/Pb ages of igneous zircon in undeformed leucogranite	(Sachan et al., 2010)
30.7	79.9	Malari	>15.2 ± 0.2	Shear zone base $^{40}Ar/^{39}Ar$ muscovite ages	(Sen et al., 2015)
29.3	80.6	Dadeldhura	>21.1--18.2	Similar $^{40}Ar/^{39}Ar$ muscovite ages in hanging wall and footwall	(Antolín et al., 2013)
30.1	81.3	Gurla Mandhata	>14--11	Initiation of faulting that cross-cuts the South Tibet detachment, from thermokinematic modeling of thermochronologic data	(McCallister et al., 2014; Murphy et al., 2002)
29.4	82.4	Bura Buri	>23.6 ± 0.8	Weighted mean of Th/Pb ages of igneous monazite in undeformed leucogranite	(Carosi et al., 2013)
28.7	83.6	Kali Gandaki	>15.5--11.8	Similar $^{40}Ar/^{39}Ar$ muscovite ages in hanging wall and footwall	(Godin et al., 2001; Vannay and Hodges, 1996)
28.6	84.3	Marsyandi Valley	<24	Youngest U/Pb ages of monazite in deformed leucocratic migmatite	(Coleman, 1998)
28.6	84.3	Marsyandi Valley	<20.1 ± 0.1	Youngest U/Pb ages of zircon in deformed leucogranite dyke	(Godin et al., 2006)
28.6	84.3	Marsyandi Valley	<18.5	Youngest U/Pb ages of monazite and zircon in locally undeformed leucogranite cut by South Tibet detachment	(Coleman, 1998; Harrison et al., 1999; Searle and Godin, 2003)
28.6	84.3	Marsyandi Valley	>19.3--14.7	Similar $^{40}Ar/^{39}Ar$ muscovite ages in hanging wall and footwall	(Copeland et al., 1990; Godin et al., 2006; Guillot et al., 1994)
29.1	84.8	Changgo	< 23.5 ± 1.0	Weighted mean of U/Pb ages of igneous zircon in deformed granite	(Larson et al., 2010)
29.1	84.8	Changgo	>18.8--17.6	Footwall and shear zone $^{40}Ar/^{39}Ar$ muscovite ages	(Larson et al., 2010)
28.5	85.0	Buri Gandaki	>13.3	Footwall $^{40}Ar/^{39}Ar$ muscovite ages	(Copeland et al., 1990)
27.8	85.0	Kathmandu Nappe	<20.0 ± 1.8	Youngest U/Pb age of zircon rim in deformed leucogranite	(Webb et al., 2011a)
27.8	85.0	Kathmandu Nappe	>15.1--12.1	Similar $^{40}Ar/^{39}Ar$ muscovite ages in hanging wall and footwall	(Arita et al., 1997; Herman et al., 2010)

29.0	85.1	Kung Tang	>16.6 ± 0.3	Weighted mean of U/Pb ages of igneous zircon in undeformed dacite	(Larson et al., 2010)
28.5	85.2	Gyirong	<23--18	Youngest U/Pb age clusters of zircon rims in deformed leucogranite samples	(Zhang et al., 2012)
28.5	85.2	Gyirong	>16.3--15.8	Footwall and shear zone $^{40}Ar/^{39}Ar$ muscovite ages	(Zhang et al., 2012)
27.8	85.5	Kathmandu Nappe	>13.8 ± 1.6	Youngest U/Pb age of zircon rim in undeformed leucogranite	(He et al., 2015)
29.0	85.5	Malashan	<17.2 ± 0.3	Youngest U/Pb age of zircon rim in deformed leucogranite	(Aoya et al., 2005)
29.0	85.5	Malashan	>17.6 ± 1.2	Youngest U/Pb age of zircon rim in undeformed leucogranite	(Zhang et al., 2012)
29.0	85.5	Malashan	>17.3--15.6	Footwall and shear zone $^{40}Ar/^{39}Ar$ muscovite ages	(Aoya et al., 2005; Zhang et al., 2012)
28.5	85.9	Xixa Pangma	<20.2 ± 0.4	Mean U/Pb age of monazite and uraninite in deformed granite	(Searle et al., 1997)
28.5	85.9	Xixa Pangma	>17.3 ± 0.4	Mean U/Pb age of monazite, uraninite, and zircon in undeformed leucogranite	(Searle et al., 1997)
28.5	85.9	Xixa Pangma	>16.7 ± 0.7	Footwall $^{40}Ar/^{39}Ar$ muscovite age	(Searle et al., 1997)
28.4	86.0	Nyalam	<17.1 ± 0.4	U/Pb zircon lower intercept age from deformed tourmaline leucogranite	(Leloup et al., 2015; Liu et al., 2012)
28.4	86.0	Nyalam	>14.1 ± 1.4	Mean U/Pb age of youngest zircon ages in undeformed leucogranite	(Wang et al., 2013)
28.4	86.0	Nyalam	>16.2--15.0	Footwall and shear zone $^{40}Ar/^{39}Ar$ muscovite ages	(Wang et al., 2006)
28.2	86.9	Everest / Rongbuk	<16.4 ± 0.1	Weighted mean of Th/Pb ages of igneous monazite in deformed leucogranite	(Cottle et al., 2015)
28.2	86.9	Everest / Rongbuk	<16.2 ± 0.8	Weighted mean of Th/Pb ages of igneous monazite in deformed leucogranite	(Murphy and Harrison, 1999)
28.2	86.9	Everest / Rongbuk	>15.6 ± 0.1	Weighted mean of Th/Pb ages of igneous monazite in undeformed leucogranite	(Cottle et al., 2015)
28.4	87.2	Dzakaa Chu	>20.4 ± 0.6	Weighted mean of Th/Pb ages of igneous monazite in undeformed leucogranite	(Cottle et al., 2007)
28.4	87.2	Dzakaa Chu	>16.7 ± 0.3	Weighted mean of Th/Pb ages of igneous monazite in undeformed leucogranite	(Cottle et al., 2007)
28.4	87.2	Dzakaa Chu	<12.8 ± 0.6	Concordia intercept age from U/Pb analyses of metamorphic titanite in deformed calc-silicate	(Cottle et al., 2011)
28.8	87.6	Lhagoi Kangri	>12.4 ± 3.6	Footwall and/or shear zone $^{40}Ar/^{39}Ar$ muscovite ages	(Maluski et al., 1988)
28.2	87.8	Saer	<16.0 ± 0.6	Average of Th/Pb ages of igneous monazite in deformed leucogranite	(Leloup et al., 2010)
28.2	87.8	Saer	>15.1 ± 0.2	Average of Th/Pb ages of igneous monazite in undeformed leucogranite	(Leloup et al., 2010)
28.2	87.8	Saer	>15.2--13.7	Footwall and shear zone base $^{40}Ar/^{39}Ar$ muscovite ages	(Hodges et al., 1994; Leloup et al., 2010; Zhang and Guo, 2007)
28.2	87.8	Saer	>11.1 ± 0.8	Average of Th/Pb ages of igneous monazite in leucogranite that cross-cuts a structure which in turn cross-cuts the South Tibet detachment shear zone	(Kali et al., 2010)
28.7	88.3	Mabja	<23.1 ± 1.6	Youngest cluster of U/Pb ages of zircon in deformed migmatite	(Lee et al., 2006)
28.7	88.3	Mabja	<21.5 ± 0.4	Youngest cluster of U/Pb ages of zircon in deformed migmatite	(Lee and Whitehouse, 2007)
28.7	88.3	Mabja	>16.2 ± 0.4	U/Pb ages of zircon in undeformed granite	(Lee and Whitehouse, 2007)
28.7	88.3	Mabja	>14.6-14.0	Youngest clusters of U/Pb ages of zircon and monazite in undeformed granite	(Lee et al., 2006; Zhang et al., 2004)
28.7	88.3	Mabja	>16.8-13.1	Footwall, shear zone, and hanging wall $^{40}Ar/^{39}Ar$ muscovite ages	(Lee et al., 2006)
28.0	88.6	Sikkim	<16--15	Youngest clusters of U/Pb ages of igneous monazite in deformed leucogranite samples	(Kellett et al., 2013)

28.0	88.6	Sikkim	<14.8 ± 0.6	Youngest Th/Pb ages of igneous monazite in deformed leucogranite	(Catlos et al., 2004; Edwards et al., 2002)
28.0	88.6	Sikkim	>15.2--13.7	Footwall and shear zone base $^{40}Ar/^{39}Ar$ muscovite ages	(Kellett et al., 2013)
28.6	88.8	Kampa	>15.5--14.7	Shear zone and immediate hanging wall $^{40}Ar/^{39}Ar$ muscovite ages	(Quigley et al., 2006)
27.4	88.9	Yadong	>12.3 ± 0.2	Footwall $^{40}Ar/^{39}Ar$ muscovite age	(Xu et al., 2013)
27.7	89.6	Lingshi klippe	<16.5 ± 0.5	Youngest U/Pb ages of igneous zircon in deformed leucogranite	(Kellett et al., 2009)
27.7	89.6	Lingshi klippe	<15.7	Youngest U/Pb ages of syn-kinematic monazite in shear zone rocks	(Kellett et al., 2010)
27.7	89.6	Lingshi klippe	>13.2--11.5	Shear zone $^{40}Ar/^{39}Ar$ muscovite ages	(Kellett et al., 2009)
28.7	89.7	Kangmar	>15.2--12.2	Shear zone $^{40}Ar/^{39}Ar$ muscovite ages	(Lee et al., 2000; Wagner et al., 2010)
28.2	89.8	Wagye La	<11.0 ± 0.5	Youngest U/Pb ages of igneous zircon and monazite in deformed leucogranite	(Kellett et al., 2009; Wu et al., 1998)
28.2	90.4	Khula Kangri	<12.5 ± 0.4	Youngest Th/Pb ages of igneous monazite in deformed leucogranite	(Edwards and Harrison, 1997)
28.2	90.4	Khula Kangri	>10.8 ± 0.8	Footwall and/or shear zone $^{40}Ar/^{39}Ar$ muscovite ages	(Maluski et al., 1988)
27.5	90.8	Ura klippe	<15.5 ± 0.5	Youngest U/Pb ages of igneous zircon in deformed leucogranite	(Kellett et al., 2009)
27.5	90.8	Ura klippe	<15.4	Youngest U/Pb ages of syn-kinematic monazite in shear zone rocks	(Kellett et al., 2010)
27.5	90.8	Ura klippe	>11.7--11.1	Shear zone $^{40}Ar/^{39}Ar$ muscovite ages	(Kellett et al., 2009)
27.4	91.7	Sakteng klippe	<24.5 ± 0.5	Weighted mean of Th/Pb ages of pre/syn-kinematic monazite in mylonitic gneiss	(Chambers et al., 2011)
27.4	91.7	Sakteng klippe	>22.7 ± 0.9	Weighted mean of Th/Pb ages of syn- and post-kinematic monazite in schist	(Chambers et al., 2011)
28.8	92.0	Yalashangbo	>20.3 ± 1.9	Mean of U/Pb ages of igneous zircon in undeformed leucogranite	(Yan et al., 2012)
28.8	92.0	Yalashangbo	>14.5--12.5	Footwall and shear zone $^{40}Ar/^{39}Ar$ muscovite ages	(Aikman et al., 2012; Yan et al., 2012; Zhang et al., 2012)

Table DR2. Timing of transition from exclusively prograde metamorphism to both prograde and retrograde metamorphism across the Greater Himalayan crystalline duplex. These findings are plotted in Figure 3.

Latitude (°N)	Longitude (°E)	Region	Timing (Ma)	Basis	Source
38.5, 28.7, 28.7	73.0, 88.3, 89.7	Pamirs, Mabja, Kangmar	23--20	Monazite: change from prograde to retrograde growth during ongoing metamorphism	(Stearns et al., 2013)
32.3	77.3	Beas	26	Zircon and monazite: prograde 41-26 Ma, retrograde 26-22 Ma	(Stübner et al., 2014)
31.3	77.4	Sutlej	<28	Monazite: prograde 42-28 Ma (1 sample)	(Webb et al., 2011b)
29.1	82.7	Dolpo	≥25.8	Monazite: prograde 43-33 Ma, retrograde at ~25.8 Ma	(Carosi et al., 2010)
28.5	83.6	Annapurna	27--23	Monazite: prograde from 48 Ma until ~27--23 Ma, retrograde growth persists until 18 Ma	(Larson and Cottle, 2015)
28.5	83.6	Annapurna	28--25	Monazite: 43-28 Ma prograde, 25-18 Ma retrograde	(Carosi et al., 2015; Iaccarino et al., 2015)
28.4	83.8	Annapurna	>22	Monazite: 38-21 Ma prograde, 22-17 Ma retrograde – but note that they didn't date the retrograde phase in the uppermost panel of the crystalline core, which elsewhere displays earliest retrograde mineral growth	(Corrie and Kohn, 2011)

28.3	84.1	Annapurna	29--22	Monazite: prograde 42-29 Ma, retrograde 22-12 Ma (~100 samples)	(Martin et al., 2007)
28.6	84.3	Marsyandi Valley	<33.2	Monazite: prograde at 33.2 Ma (one sample)	(Catlos et al., 2001)
27.8	87.8	Far-east Nepal	26--24	Monazite: 42-26 Ma prograde, 24--13 Ma retrograde (structurally lower samples show younger transition)	(Ambrose et al., 2015)
27.0	88.3	Sikkim	26--20	Monazite: 40-26 Ma prograde, 20 Ma retrograde	(Mottram et al., 2014)
27.7	88.6	Sikkim	27	Zircon and monazite: 31-27 prograde, 27-17 retrograde	(Rubatto et al., 2013)
27.6	91.2	East Bhutan	27--26	Zircon and monazite: 36-27 prograde, 26-13 retrograde	(Zeiger et al., 2015)

Table DR3. Timing of decompression and cooling across the structurally high (northern) portions of the Greater Himalayan crystalline duplex.

Lat. (°N)	Lon. (°E)	Region	Pressure$_1$ (GPa)	Pressure$_2$ (GPa)	Temp$_1$ (°C)	Temp$_2$ (°C)	Time$_1$ (Ma)	Time$_2$ (Ma)	Comments	Source
33.0	77.2	SE Zanskar			≥550	440--390	22--21	22.1--19.3		(Dézes et al., 1999; Horton et al., 2015; Walker et al., 1999)
33.0	77.2	SE Zanskar			440--390	195--175	22.1--19.3	12.3--11.4		(Deeken et al., 2011; Dézes et al., 1999; Horton et al., 2015; Walker et al., 1999)
32.3	77.2	Beas	0.7--0.5	0.4--0.2	≥650	440--390	26--23	22.2--20.6		(Schlup et al., 2011; Stübner et al., 2014; Walker et al., 1999)
32.3	77.2	Beas			440--390	280--200	22.2--20.6	12--8		(Schlup et al., 2011; Stübner et al., 2014; Walker et al., 1999)
31.0	79.0	Gangotri			≥550	440--390	23.0 ± 0.4	17.9 ± 0.1		(Searle et al., 1999; Sorkhabi et al., 1996)
31.0	79.0	Gangotri			440--390	130--90	17.9 ± 0.1	2.4--1.5		(Sorkhabi et al., 1996)
30.7	79.9	Malari			≥550	440--390	18.9 ± 0.6	15.2 ± 0.2		(Sachan et al., 2010; Sen et al., 2015)
28.6	84.3	Marsyandi Valley			≥550	440--390	≥18.5	19.3--14.7		(Coleman, 1998; Copeland et al., 1990; Godin et al., 2006; Guillot et al., 1994; Harrison et al., 1999; Searle and Godin, 2003)
28.6	84.3	Marsyandi Valley			440--390	280--200	19.3--14.7	2--1		(Blythe et al., 2007; Coleman, 1998; Copeland et al., 1990; Godin et al., 2006; Guillot et al., 1994; Searle and Godin, 2003)
28.5	85.9	Xixa Pangma			≥550	440--390	17.3 ± 0.4	16.7 ± 0.7		(Searle et al., 1997)

28.5	85.9	Xixa Pangma			440--390	130--90	16.7 ± 0.7	14.8--12.3		(Searle et al., 1997)
28.4	86.0	Nyalam			≥550	440--390	17.1--14.1	16.2--15.0		(Leloup et al., 2015; Liu et al., 2012; Wang et al., 2013; Wang et al., 2006)
28.4	86.0	Nyalam			440--390	200	16.2--15.0	14.3--13.9		(Liu et al., 2012; Wang et al., 2006)
28.4	86.0	Nyalam			200	130--90	14.3--13.9	14--10		(Liu et al., 2012)
28.2	86.9	Everest / Rongbuk	0.70--0.55	0.4--0.2	680--550	630--550	32	24		(Jessup et al., 2008)
28.2	86.9	Everest / Rongbuk			630--550	440--390	15.6--15.3	14--13		(Cottle et al., 2015; Jessup et al., 2008; Schultz et al., 2014)
28.2	86.9	Everest / Rongbuk			440--390	240--190	15.5--14.2	14.5--11		(Schultz et al., 2014)
28.2	87.4	Ama Drime	>1.5	1.0--0.8	>580	750	38	15--13		(Kellett et al., 2014)
28.2	87.4	Ama Drime	1.0--0.8	0.4	750	750	15--13	13		(Cottle et al., 2009; Kellett et al., 2014)
28.2	87.4	Ama Drime			750	300	13	13--10		(Cottle et al., 2009; Kali et al., 2010; Kellett et al., 2014)
27.8	87.4	Arun Valley	>1.5	1.2	670	780	26--23	23--13	This is somewhat south of the GHC-north	(Corrie et al., 2010)
27.8	87.4	Arun Valley	1.2	0.6	780	675	23--13	14--13	This is somewhat south of the GHC-north	(Corrie et al., 2010)
28.2	87.8	Sa'er			700	150	15--13	15--13		(Hodges et al., 1994; Kali et al., 2010; Leloup et al., 2010)
27.7	88.6	Sikkim	1.2--0.9	0.5--0.3	800--750	800--750	23	20		(Rubatto et al., 2013; Sorcar et al., 2014)
27.7	88.6	Sikkim	0.5--0.3	0.5--0.3	800--750	600	20	17		(Rubatto et al., 2013; Sorcar et al., 2014)
28.0	88.6	Sikkim			750-650	130--90	15	13		(Kellett et al., 2013)
27.7	89.5	Lingshi			700--550	440--390	16.5	13.2--11.5		(Kellett et al., 2009)
27.7	89.5	Lingshi			440--390	130--90	13.2--11.5	6--4		(Grujic et al., 2006; Kellett et al., 2009)
28.1	89.7	NW Bhutan	>1.5	1.0--0.8	760	800--750	15.3--14.4	13.9		(Grujic et al., 2011; Warren et al., 2011)
28.1	89.7	NW Bhutan			800--750	680--580	13.9	11--10		(Warren et al., 2012; Warren et al., 2011)
28.2	90.4	Khula Kangri			≥550	440--390	12.5 ± 0.4	10.8 ± 0.8		(Edwards and Harrison, 1997)
27.5	90.9	Ura			600--500	440--390	15.5	11.1	This is somewhat south of the GHC-north	(Kellett et al., 2009)
27.5	90.9	Ura			440--390	130--90	11.1	8--6	This is somewhat south of the GHC-north	(Grujic et al., 2006; Kellett et al., 2009)
27.6	91.7	NW Arunachal			700--550	440--390	12.7--11.5	9--7	Along an out-of-sequence thrust	(Mathew et al., 2013; Warren et al., 2014)

29.7	94.9	Eastern Himalayan Syntaxis	1.8--1.4	1.0--0.8	800	800--900	24	19		(Xu et al., 2010b)
29.7	94.9	Eastern Himalayan Syntaxis	1.0--0.8	0.60--0.45	900--800	700--650	19	17		(Xu et al., 2010b)

Table DR4. Literature sources constraining a cooling pulse migrating across the Himalayan hinterland, as constrained by foreland basin thermochronologic records. See Figure 4 and Figure DR1 for data plots and interpretations.

Latitude (°N)	Longitude (°E)	Region	Basis	Source
32.7	72.5	Western Himalayan foreland (Chinji)	Zircon fission track detrital thermochronology	(Cerveny et al., 1988; Chirouze et al., 2015)
32.7	72.5	Western Himalayan foreland (Chinji)	Ar-Ar muscovite detrital thermochronology	(Najman et al., 2003)
31	77	Western Himalayan foreland (Jogindernagar)	Ar-Ar muscovite detrital thermochronology	(Najman et al., 1997)
30.8	77	Western Himalayan foreland (Jogindernagar)	Zircon fission track detrital thermochronology	(Jain et al., 2009)
31.8	76.7	Western Himalayan foreland (Jawalamukhi)	Ar-Ar muscovite detrital thermochronology	(Najman et al., 2009; White et al., 2002)
31.8	76.7	Western Himalayan foreland (Kangra)	Zircon fission track detrital thermochronology	(Najman et al., 2004)
29.1	81.7	Central Himalayan foreland (Karnali)	Zircon fission track detrital thermochronology	(Bernet et al., 2006)
29.1	81.7	Central Himalayan foreland (Karnali)	Ar-Ar muscovite detrital thermochronology	(Szulc et al., 2006)
27.7	82.8	Central Himalayan foreland (Surai Khola)	Zircon fission track detrital thermochronology	(Bernet et al., 2006)
27.8	83.5	Central Himalayan foreland (Tinau Khola)	Zircon fission track detrital thermochronology	(Bernet et al., 2006)
27.7	82.8	Central Himalayan foreland (Surai Khola)	Ar-Ar muscovite detrital thermochronology	(Szulc et al., 2006)
27.8	83.5	Central Himalayan foreland (Tinau Khola)	Ar-Ar muscovite detrital thermochronology	(Szulc et al., 2006)
27.5	87	Eastern Himalayan foreland (Muksar Khola)	Zircon fission track detrital thermochronology	(Chirouze et al., 2012)
27.5	92.5	Eastern Himalayan foreland (Kameng)	Zircon fission track detrital thermochronology	(Chirouze et al., 2013)

Table DR5. Published interpretations of synchronous Indian slab detachment along the length of the Himalaya, as discussed in the text.

Latitude	Longitude	Region	Timing (Ma)	Basis	Source
38.5, 28.7, 28.7	73.0, 88.3, 89.7	Pamirs, Mabja, Kangmar	23--20	Change from prograde to retrograde monazite growth during ongoing metamorphism	(Stearns et al., 2013)
35.8	75.7	South Karakoram	25--21	Metamorphism and Baltoro granite emplacement may signify heating from slab detachment	(Rolland et al., 2001)
35.9	75.8	South Karakoram	~25	Geochemistry of ~25 Ma volcanic rocks	(Mahéo et al., 2002)
28.0	79.5	Central Himalayan foreland	~15	Shift in the foreland basin southwards propagation rate, pre-Siwalik to Siwalik transition (i.e., onset of major molasse deposition)	(Mugnier and Huyghe, 2006)
28.0	82.5	Central Himalayan foreland	~16	Detrital thermochronology in the foreland basin records a rapid cooling (and inferred uplift) event in the hinterland	(Bernet et al., 2006)
27.8	87.4	Arun Valley	~25	Pulse of heating experienced by deep rocks: eclogite metamorphism at ~26-23 Ma followed by granulite metamorphism at ~15-13 Ma	(Corrie et al., 2010)
29.7	94.9	East Himalayan Syntaxis	~24	Heating indicated by granulite facies metamorphism	(Xu et al., 2010b)

Table DR6. Compilation of timing constraints for high-potassium (high-K) and adakitic magmatism across southern Tibet. These data are plotted in Figures 2 and 3.

Latitude	Longitude	Region	Timing (Ma)	Lithology	Basis	Source
33.8	78.1	Pangong	19.1--16.6	Adakitic	Zircon U-Pb ages	(Ravikant et al., 2009)
32.4	80.1	Shiquanhe	24--16	High-K	Phlogopite, biotite, and whole rock Ar/Ar ages	(Arnaud et al., 1992; Turner et al., 1996; Williams et al., 2004)
32.38	80.31	Shiquanhe	22.6 ± 0.2	High-K	Biotite Ar/Ar age	(Kapp et al., 2003)
31.0	81.0	Bangba	17.01 ± 0.23	Adakitic	Zircon U-Pb age	(Chen et al., 2011)
32.0	81.2	Manasarowar	17--16.7	High-K	Plagioclase and Biotite Ar/Ar ages	(Miller et al., 1999)
32.0	81.2	Southern Bongba	25.4--23.3	High-K	Whole rock Ar/Ar ages	(Miller et al., 1999)
31.0	81.5	Kailas	16.9 ± 0.4	High-K	Plagioclase Ar/Ar age	(Aitchison et al., 2009)
31.0	81.5	Kailas	24.6--24.17	Adakitic	Zircon U-Pb ages	(DeCelles et al., 2011)
32.1	81.6	Xungba	23.4 ± 0.1	High-K	Zircon U-Pb ages	(Liu et al., 2014a)
31.5	81.7	Gegar	17.7--16.2	High-K	Zircon U-Pb ages	(Miller et al., 1999)
31.9--32.0	81.8--82.1	Xungba	23.3--21	High-K	Phlogopite and matrix Ar/Ar ages, and zircon U-Pb ages	(Liu et al., 2014a; Miller et al., 1999)
32.0	81.8	Southern Xungba	22.8--18.1	High-K	Phlogopite and whole rock Ar/Ar ages	(Miller et al., 1999)
32.0	81.8	Eastern Jarga	18.5--15.5	High-K	Phlogopite and matrix Ar/Ar ages	(Miller et al., 1999)
31.3	82.1	Yare	16.8 ± 0.8	Adakitic	Zircon U-Pb age	(Hou et al., 2013)
32.0	82.3	Bangba	23.5--23.3	High-K	Zircon U-Pb age	(Liu et al., 2014b)
31.3	82.3	Mayum	18.4--17.68	High-K	Biotite Ar/Ar age and Zircon U-Pb age	(Jiang et al., 2009; Jiang et al., 2006)
31.5	82.8	Dawacuo, Zabuye, Maige, Anglarencuo	17.47--15.82	High-K	Biotite Ar/Ar age	(Ding et al., 2006)
31.3	83.0	Sailipu	17.58 ± 0.19	High-K	Phlogopite Ar/Ar age	(Wang et al., 2008)
31.3	83.0	Sailipu	17.1--16.2	High-K	Zircon U-Pb ages	(Sun et al., 2007)
31.4	84.3	Zabuye	16.16--15.56	High-K	Biotite, sanidine, and whole rock Ar/Ar ages	(Nomade et al., 2004)
30.8	84.4	Gongmutang	16.59--16.1	High-K	Sanidine Ar/Ar ages	(Zhao et al., 2009)
33.1	85.1	Qiangtang	30.5 ± 0.12	High-K	Whole rock Ar/Ar age	(Li et al., 2006)
32.6	85.4	Qiangtang	35.9 ± 0.6	High-K	Hornblende Ar/Ar age	(Ding et al., 2007)
30.0	85.6	Daggyar Tso	19.3--17.3	High-K	Phlogopite, Hb, and whole rock Ar/Ar ages	(Williams et al., 2001)
30.5	86.0	Xuru lake	11.5 ± 0.2	High-K	Biotite Ar/Ar ages	(Zhao et al., 2006)
30.5	86.0	Konglongxiang	21.38 ± 0.11	High-K	Whole rock Ar/Ar ages	(Chen et al., 2010)

30.9	86.4	Dangreyong cuo	14.2--13.4	High-K	Biotite and sanidine Ar/Ar ages	(Zhao et al., 2006)
30.0	86.5	Pabbai Zong	18.3--13.3	High-K	Phlogopite Ar/Ar age	(Williams et al., 2001)
31.1	86.5	Yulinshan	22.9 ± 0.14	High-K	Sanidine Ar/Ar age	(Ding et al., 2003)
30.1	86.6	Chazi	11.7 ± 0.3	High-K	Zircon U-Pb age	(Guo et al., 2013)
30.0	86.6	Chazi	13.6--8.2	High-K	Biotite, sanidine, and phlogopite Ar/Ar ages	(Ding et al., 2003; Ding et al., 2006)
31.0	86.6	Wenbu	13.3--13.1	High-K	Sanidine Ar/Ar age	(Ding et al., 2003)
30.9	86.6	Mibale	12.6 ± 1.94	High-K	K-Ar age	(Liao et al., 2002)
32.2	86.8	Qiangtang	34.2 ± 0.2	High-K	Sanidine Ar/Ar age	(Ding et al., 2007)
29.5	87.4	Zhuno	15.6 ± 0.6	Adakitic	Zircon U-Pb age	(Gao et al., 2010; Zheng et al., 2007)
29.3	88.0	Xigaze	18.3--14	High-K	Sanidine, K-feldspar, and bh Ar/Ar ages	(Yin et al., 1994)
29.8	88.3	Nanmuqie	14.4--14.3	Adakitic	Zircon U-Pb ages	(Xu et al., 2010a)
29.0	88.4	Kuday	11.49--9.13	Adakitic	Biotite Ar/Ar and Zircon U-Pb ages	(King et al., 2007)
29.4	88.8	Xigaze	15 ± 1.2	High-K	Whole rock Ar/Ar age	(Chung et al., 2003)
29.3	88.9	Xigaze	18.4 ± 1.6	High-K	Whole rock Ar/Ar age	(Chung et al., 2003)
29.4	89.0	Wuyu, Namulin	14.71--10.47	High-K	Biotite, K-feldspar, sanidine, and plagioclase Ar/Ar ages	(Zhou, 2002)
29.7	89.0	Pagu	14.6--14	Adakitic	Zircon U-Pb ages	(Xu et al., 2010a)
29.4	89.5	Namulin	13.9--12.5	High-K	Biotite Ar/Ar ages	(Williams et al., 2004)
29.7	89.6	Wuyu Basin	13.63--11.09	High-K	K-feldspar, biotite, and plagioclase Ar/Ar ages	(Zhou et al., 2010)
29.7	89.6	Namulin	15.03--14.03	High-K	sanidine Ar/Ar ages	(Spicer et al., 2003)
29.3	89.6	Dazhuqu	22.2--19.5	High-K	Biotite and plagioclase Ar/Ar ages	(Aitchison et al., 2009)
29.6	89.6	Chongjiang	15.6--14.5	Adakitic	Zircon U-Pb ages	(Hou et al., 2004)
29.7	89.6	Namulin	15.25--15.1	High-K	Sanidine Ar/Ar ages	(Spicer et al., 2003)
29.7	89.7	Dangxiong	15.48 ± 0.22	High-K	plagioclase Ar/Ar age	(Zhou et al., 2010)
19.9	89.9	MaQiang	15.8--14.4	High-K	Biotite and Hb Ar/Ar ages	(Coulon et al., 1986)
29.5	89.9	Bairong, Tinggong	16--14.2	Adakitic	Zircon U-Pb ages	(Li et al., 2011)
29.6	90.0	Chongjiang	12.22 ± 0.05	High-K	plagioclase Ar/Ar age	(Qu et al., 2003)
29.5	90.0	Majiang, Nymo	15.1--14.9	Adakitic	Zircon U-Pb ages	(Chung et al., 2009; Ji et al., 2009)
29.6	90.0	Chongjiang	15.3--13.5	Adakitic	Biotite Ar/Ar and Zircon U-Pb ages	(Ji et al., 2009; Qu et al., 2003)
29.7	90.4	Dangxiong	11.4--10.32	High-K	Biotite and sanidine Ar/Ar ages	(Zhou et al., 2010)
29.5	90.4	Yangying	10.88--10.6	High-K	Biotite and sanidine Ar/Ar ages	(Nomade et al., 2004)
29.4	90.7	Baijin	21.3 ± 1.2	Adakitic	Zircon U-Pb age	(Ji et al., 2009)
29.5	90.8	Nanmu, Nemu	17.7--12.75	Adakitic	Zircon U-Pb ages	(Chen et al., 2011; Ji et al., 2009)

29.5	90.9	Jiama	16.6--15.46	Adakitic	Zircon U-Pb, sanidine and whole rock Ar/Ar ages	(Chen et al., 2011; Chung et al., 2003)
29.5	91.2	Qiangdui	19.1--17.1	Adakitic	Zircon U-Pb ages	(Li et al., 2011)
29.6	91.3	Lakang'e	13.42--12.5	High-K	Biotite and plagioclase Ar/Ar ages	(Qu et al., 2003)
26.7	91.8	Jiama	15--13.2	Adakitic	Zircon U-Pb age and whole rock Ar/Ar age	(Chung et al., 2003)
29.3	91.9	Yaja, Chongmuda, sanidinegri, Mingze	31.7--28.5	Adakitic	Zircon U-Pb ages	(Chung et al., 2009; Harrison et al., 2000; Jiang et al., 2014; Zhang et al., 2014; Zheng et al., 2012b)
29.6	93.0	Tangbula	19.2 ± 0.2	Adakitic	Zircon U-Pb age	(Wang et al., 2010)
29.6	94.3	Bayi	22 ± 2	Adakitic	Zircon U-Pb age	(Zhang et al., 2010)
29.6	94.4	Dangru	25.7 ± 0.3	Adakitic	Zircon U-Pb age	(Zhang et al., 2014)
30.0	94.6	Lunan	25.4 ± 0.6	Adakitic	Zircon U-Pb age	(Zhang et al., 2010)
29.6	94.7	Linzhi	27.1--26	Adakitic	Zircon U-Pb ages	(Booth et al., 2004; Chung et al., 2003; Zhang et al., 2014; Zheng et al., 2012a)
29.4	95.3	Beibeng	29.9--27.5	Adakitic	Zircon U-Pb ages	(Pan et al., 2012)
29.5	95.4	Damu, Lengduo	28.5--26.1	Adakitic	Zircon U-Pb ages	(Pan et al., 2012; Zhang et al., 2014)
29.6	95.5	Balonggong	27.1--26.5	Adakitic	Zircon U-Pb ages	(Pan et al., 2012)
29.8	95.7	Bomi	23.7 ± 0.5	Adakitic	Zircon U-Pb ages	(Pan et al., 2012)

References Cited in Data Repository.

Aikman, A., Harrison, T., and Hermann, J., 2012, Age and thermal history of Eo- and Neohimalayan granitoids, eastern Himalaya: Journal of Asian Earth Sciences, v. 51, p. 85–97.

Aitchison, J., Ali, J., Chan, A., Davis, A., and Lo, C.-H., 2009, Tectonic implications of felsic tuffs within the Lower Miocene Gangrinboche conglomerates, southern Tibet: Journal of Asian Earth Sciences, v. 34, no. 3, p. 287–297.

Ambrose, T. K., Larson, K. P., Guilmette, C., Cottle, J. M., Buckingham, H., and Rai, S., 2015, Lateral extrusion, underplating, and out-of-sequence thrusting within the Himalayan metamorphic core, Kanchenjunga, Nepal: Lithosphere, v. 7, no. 4, p. 441-464.

Antolín, B., Godin, L., Wemmer, K., and Nagy, C., 2013, Kinematics of the Dadeldhura klippe shear zones (W Nepal): implications for the foreland evolution of the Himalayan metamorphic core: Terra Nova, v. 25, no. 4, p. 282-291.

Aoya, M., Wallis, S. R., Terada, K., Lee, J., Kawakami, T., Wang, Y., and Heizler, M., 2005, North-south extension in the Tibetan crust triggered by granite emplacement: Geology, v. 33, no. 11, p. 853-856.

Arita, K., Dallmeyer, R. D., and Takasu, A., 1997, Tectonothermal evolution of the Lesser Himalaya, Nepal: Constraints from 40Ar/39Ar ages from the Kathmandu Nappe: The Island Arc, v. 6, p. 372–385.

Arnaud, N. O., Vidal, P., Tapponnier, P., Matte, P., and Deng, W. M., 1992, The high K2O volcanism of northwestern Tibet: Geochemistry and tectonic implications: Earth and Planetary Science Letters, v. 111, no. 2-4, p. 351-367.

Bernet, M., van der Beek, P., Pik, R., Huyghe, P., Mugnier, J.-L., Labrin, E., and Szulc, A., 2006, Miocene to Recent exhumation of the central Himalaya determined from combined detrital zircon fission-track and U/Pb analysis of Siwalik sediments, western Nepal: Basin Research, v. 18, no. 4, p. 393–412.

Blythe, A. E., Burbank, D. W., Carter, A., Schmidt, K., and Putkonen, J., 2007, Plio-Quaternary exhumation history of the central Nepalese Himalaya: 1. Apatite and zircon fission track and apatite [U-Th]/He analyses: Tectonics, v. 26, no. 3.

Booth, A. L., Zeitler, P. K., Kidd, W. S. F., Wooden, J., Liu, Y., Idleman, B., Hren, M., and Chamberlain, C. P., 2004, U-Pb zircon constraints on the tectonic evolution of southeastern Tibet, Namche Barwa Area: American Journal of Science, v. 304, no. 10, p. 889–929.

Carosi, R., Montomoli, C., Langone, A., Turina, A., Cesare, B., Iaccarino, S., Fascioli, L., Visonà, D., Ronchi, A., and Rai, S., 2015, Eocene partial melting recorded in peritectic garnets from kyanite-gneiss, Greater Himalayan Sequence, central Nepal: Geological Society, London, Special Publications, v. 412, no. 1, p. 111-129.

Carosi, R., Montomoli, C., Rubatto, D., and Visonà, D., 2010, Late Oligocene high-temperature shear zones in the core of the Higher Himalayan Crystallines (Lower Dolpo, western Nepal): Tectonics, v. 29, no. 4.

Carosi, R., Montomoli, C., Rubatto, D., and Visonà, D., 2013, Leucogranite intruding the South Tibetan Detachment in western Nepal: implications for exhumation models in the Himalayas: Terra Nova, v. 25, no. 6, p. 478-489.

Catlos, E., Dubey, C., Harrison, T., and Edwards, M., 2004, Late Miocene movement within the Himalayan Main Central Thrust shear zone, Sikkim, north-east India: Journal of Metamorphic Geology, v. 22, no. 3, p. 207–226.

Catlos, E. J., Harrison, T. M., Kohn, M. J., Grove, M., Ryerson, F. J., Manning, C. E., and Upreti, B. N., 2001, Geochronologic and thermobarometric constraints on the evolution of the Main Central Thrust, central Nepal Himalaya: Journal of Geophysical Research-Solid Earth, v. 106, p. 16177–16204.

Cerveny, P. F., Naeser, N. D., Zeitler, P. K., Naeser, C. W., and Johnson, N. M., 1988, History of uplift and relief of the Himalaya during the past 18 million years: evidence from fission-track ages of detrital zircons from sandstones of the Siwalik Group: Springer, p. 43-61.

Chambers, J., Parrish, R., Argles, T., Harris, N., and Horstwood, M., 2011, A short-duration pulse of ductile normal shear on the outer South Tibetan detachment in Bhutan: Alternating channel flow and critical taper mechanics of the eastern Himalaya: Tectonics, v. 30, no. 2.

Chen, J.-l., Xu, J.-f., Wang, B.-d., Kang, Z.-q., and Jie, L., 2010, Origin of Cenozoic alkaline potassic volcanic rocks at KonglongXiang, Lhasa terrane, Tibetan Plateau: Products of partial melting of a mafic lower-crustal source?: Chemical Geology, v. 273, no. 3-4, p. 286-299.

Chen, J.-L., Xu, J.-F., Zhao, W.-X., Dong, Y.-H., Wang, B.-D., and Kang, Z.-Q., 2011, Geochemical variations in Miocene adakitic rocks from the western and eastern Lhasa terrane: Implications for lower crustal flow beneath the Southern Tibetan Plateau: Lithos, v. 125, no. 3-4, p. 928-939.

Chirouze, F., Bernet, M., Huyghe, P., Erens, V., Dupont-Nivet, G., and Senebier, F., 2012, Detrital thermochronology and sediment petrology of the middle Siwaliks along the Muksar Khola section in eastern Nepal: Journal of Asian Earth Sciences, v. 44, p. 289-301.

Chirouze, F., Huyghe, P., Chauvel, C., Beek, P., Bernet, M., and Mugnier, J.-L., 2015, Stable Drainage Pattern and Variable Exhumation in the Western Himalaya since the Middle Miocene: The Journal of Geology, v. 123, no. 1, p. 1-20.

Chirouze, F., Huyghe, P., van der Beek, P., Chauvel, C., Chakraborty, T., Dupont-Nivet, G., and Bernet, M., 2013, Tectonics, exhumation, and drainage evolution of the eastern Himalaya since 13 Ma from detrital geochemistry and thermochronology, Kameng River Section, Arunachal Pradesh: Geological Society of America Bulletin, v. 125, no. 3-4, p. 523-538.

Chung, S.-L., Chu, M.-F., Ji, J., O'Reilly, S. Y., Pearson, N. J., Liu, D., Lee, T.-Y., and Lo, C.-H., 2009, The nature and timing of crustal thickening in Southern Tibet: Geochemical and zircon Hf isotopic constraints from postcollisional adakites: Tectonophysics, v. 477, no. 1-2, p. 36-48.

Chung, S.-L., Liu, D., Ji, J., Chu, M.-F., Lee, H.-Y., Wen, D.-J., Lo, C.-H., Lee, T.-Y., Qian, Q., and Zhang, Q., 2003, Adakites from continental collision zones: Melting of thickened lower crust beneath southern Tibet: Geology, v. 31, no. 11, p. 1021-1024.

Coleman, M. E., 1998, U-Pb constraints on Oligocene-Miocene deformation and anatexis within the central Himalaya, Marsyandi valley, Nepal: American Journal of Science, v. 298, p. 553-571.

Copeland, P., Harrison, T., and Fort, P., 1990, Age and cooling history of the Manaslu granite: implications for Himalayan tectonics: Journal of Volcanology and Geothermal Research, v. 44, no. 1-2, p. 33-50.

Corrie, S. L., and Kohn, M. J., 2011, Metamorphic history of the central Himalaya, Annapurna region, Nepal, and implications for tectonic models: Geological Society of America Bulletin, v. 123, no. 9-10, p. 1863-1879.

Corrie, S. L., Kohn, M. J., and Vervoort, J. D., 2010, Young eclogite from the Greater Himalayan Sequence, Arun Valley, eastern Nepal: P–T–t path and tectonic implications: Earth and Planetary Science Letters, v. 289, no. 3-4, p. 406–416.

Cottle, J., Jessup, M., Newell, D., Searle, M., Law, R., and Horstwood, M., 2007, Structural insights into the early stages of exhumation along an orogen-scale detachment: The South Tibetan Detachment System, Dzakaa Chu section, Eastern Himalaya: Journal of Structural Geology, v. 29, no. 11, p. 1781–1797.

Cottle, J. M., Jessup, M. J., Newell, D. L., Horstwood, M. S. A., Noble, S. R., Parrish, R. R., Waters, D. J., and Searle, M. P., 2009, Geochronology of granulitized eclogite from the Ama Drime Massif: Implications for the tectonic evolution of the South Tibetan Himalaya: Tectonics, v. 28.

Cottle, J. M., Searle, M. P., Jessup, M. J., Crowley, J. L., and Law, R. D., 2015, Rongbuk re-visited: Geochronology of leucogranites in the footwall of the South Tibetan Detachment System, Everest Region, Southern Tibet: Lithos, v. 227, p. 94-106.

Cottle, J. M., Waters, D. J., Riley, D., Beyssac, O., and Jessup, M. J., 2011, Metamorphic history of the South Tibetan Detachment System, Mt. Everest region, revealed by RSCM thermometry and phase equilibria modelling: Journal of Metamorphic Geology, v. 29, no. 5, p. 561–582.

Coulon, C., Maluski, H., Bollinger, C., and Wang, S., 1986, Mesozoic and Cenozoic volcanic rocks from central and southern Tibet: 39Ar-40Ar dating, petrological characteristics and geodynamical significance: Earth and Planetary Science Letters, v. 79, p. 281-302.

DeCelles, P. G., Kapp, P., Quade, J., and Gehrels, G. E., 2011, Oligocene-Miocene Kailas basin, southwestern Tibet: Record of postcollisional upper-plate extension in the Indus-Yarlung suture zone: Geological Society of America Bulletin, v. 123, no. 7-8, p. 1337–1362.

Deeken, A., Thiede, R. C., Sobel, E. R., Hourigan, J. K., and Strecker, M. R., 2011, Exhumational variability within the Himalaya of northwest India: Earth and Planetary Science Letters, v. 305, no. 1-2, p. 103–114.

Dézes, P., Vannay, J. C., Steck, A., Bussy, F., and Cosca, M., 1999, Synorogenic extension: Quantitative constraints on the age and displacement of the Zanskar shear zone (northwest Himalaya): Geological Society of America Bulletin, v. 111, no. 3, p. 364–374.

Ding, L., Kapp, P., Yue, Y., and Lai, Q., 2007, Postcollisional calc-alkaline lavas and xenoliths from the southern Qiangtang terrane, central Tibet: Earth and Planetary Science Letters, v. 254, no. 1-2, p. 28–38.

Ding, L., Kapp, P., Zhong, D., and Deng, W., 2003, Cenozoic Volcanism in Tibet: Evidence for a Transition from Oceanic to Continental Subduction: Journal of Petrology, v. 44, no. 10, p. 1833-1865.

Ding, L., Yue, Y., Cai, F., Xu, X., Zhang, Q., and Lai, Q., 2006, 40Ar/39Ar geochronology, geochemical, Sr–Nd–O isotopic characteristics of the high-Mg ultrapotassic rocks in Lhasa block of Tibet: implications in the onset time, depth of NS-striking rift system: Acta Geologica Sinica, v. 80, p. 1252-1261.

Edwards, M. A., Catlos, E. J., Harrison, T. M., and Dubey, C. S., 2002, We seek him now, we sought him then: Seventy years of constraints on the STDS in Sikkim: Journal of Asian Earth Sciences, v. 20, no. 4S1.

Edwards, M. A., and Harrison, T. M., 1997, When did the roof collapse? Late Miocene north-south extension in the high Himalaya revealed by Th-Pb monazite dating of the Khula Kangri granite: Geology, v. 25, no. 6, p. 543-546.

Gao, Y., Yang, Z., Santosh, M., Hou, Z., Wei, R., and Tian, S., 2010, Adakitic rocks from slab melt-modified mantle sources in the continental collision zone of southern Tibet: Lithos, v. 119, no. 3-4, p. 651-663.

Godin, L., Gleeson, T., Searle, M., Ullrich, T., and Parrish, R., 2006, Locking of southward extrusion in favour of rapid crustal-scale buckling of the Greater Himalayan sequence, Nar valley, central Nepal: Geological Society, London, Special Publications, v. 268, no. 1, p. 269-292.

Godin, L., Parrish, R. R., Brown, R. L., and Hodges, K. V., 2001, Crustal thickening leading to exhumation of the Himalayan metamorphic core of central Nepal: Insight from U-Pb geochronology and 40Ar/39Ar thermochronology: Tectonics, v. 20, no. 5, p. 729–747.

Grujic, D., Coutand, I., Bookhagen, B., Bonnet, S., Blythe, A., and Duncan, C., 2006, Climatic forcing of erosion, landscape, and tectonics in the Bhutan Himalayas: Geology, v. 34, no. 10, p. 801-804.

Grujic, D., Warren, C. J., and Wooden, J. L., 2011, Rapid synconvergent exhumation of Miocene-aged lower orogenic crust in the eastern Himalaya: Lithosphere, v. 3, no. 5, p. 346-366.

Guillot, S., Hodges, K., Le Fort, P., and Pecher, A., 1994, New constraints on the age of the Manaslu leucogranite: Evidence for episodic tectonic denudation in the central Himalayas: Geology, v. 22, p. 559-562.

Guo, Z., Wilson, M., Zhang, M., Cheng, Z., and Zhang, L., 2013, Post-collisional, K-rich mafic magmatism in south Tibet: constraints on Indian slab-to-wedge transport processes and plateau uplift: Contributions to Mineralogy and Petrology, v. 165, no. 6, p. 1311–1340.

Harrison, M., Grove, M., McKeegan, K., Coath, C., Lovera, O., and Fort, P., 1999, Origin and Episodic Emplacement of the Manaslu Intrusive Complex, Central Himalaya: Journal of Petrology, v. 40, no. 1, p. 3-19.

Harrison, T. M., Yin, A., Grove, M., Lovera, O. M., Ryerson, F. J., and Zhou, X., 2000, The Zedong Window: A record of superposed Tertiary convergence in southeastern Tibet: Journal of Geophysical Research, v. 105, no. B8, p. 19211–19230.

He, D., Webb, A. A. G., Larson, K. P., Martin, A. J., and Schmitt, A. K., 2015, Extrusion vs. duplexing models of Himalayan mountain building 3: duplexing dominates from the Oligocene to Present: International Geology Review, v. 57, no. 1, p. 1-27.

Herman, F., Copeland, P., Avouac, J.-P., Bollinger, L., Mahéo, G., Fort, P., Rai, S., Foster, D., Pêcher, A., Stüwe, K., and Henry, P., 2010, Exhumation, crustal deformation, and thermal structure of the Nepal Himalaya derived from the inversion of thermochronological and thermobarometric data and modeling of the topography: Journal of Geophysical Research, v. 115, no. B6.

Hodges, K., Hames, W., Olszewski, W., Burchfiel, B., Royden, L., and Chen, Z., 1994, Thermobarometric and40Ar/39Ar geochronologic constraints on Eohimalayan metamorphism in the Dinggyê area, southern Tibet: Contributions to Mineralogy and Petrology, v. 117, no. 2, p. 151–163.

Horton, F., Lee, J., Hacker, B., Bowman-Kamaha'o, M., and Cosca, M., 2015, Himalayan gneiss dome formation in the middle crust and exhumation by normal faulting: New

geochronology of Gianbul dome, northwestern India: Geological Society of America Bulletin, v. 127, no. 1-2, p. 162-180.

Hou, Z., Zheng, Y., Yang, Z., Rui, Z., Zhao, Z., Jiang, S., Qu, X., and Sun, Q., 2013, Contribution of mantle components within juvenile lower-crust to collisional zone porphyry Cu systems in Tibet: Mineralium Deposita, v. 48, no. 2, p. 173–192.

Hou, Z. Q., Gao, Y. F., Qu, X. M., Rui, Z. Y., and Mo, X. X., 2004, Origin of adakitic intrusives generated during mid-Miocene east–west extension in southern Tibet: Earth and Planetary Science Letters, v. 220, no. 1-2, p. 139–155.

Iaccarino, S., Montomoli, C., Carosi, R., Massonne, H.-J., Langone, A., and Visonà, D., 2015, Pressure–temperature–time–deformation path of kyanite-bearing migmatitic paragneiss in the Kali Gandaki valley (Central Nepal): Investigation of Late Eocene–Early Oligocene melting processes: Lithos, v. 231, p. 103-121.

Jain, A. K., Lal, N., Sulemani, B., Awasthi, A. K., Singh, S., Kumar, R., and Kumar, D., 2009, Detrital-zircon fission-track ages from the Lower Cenozoic sediments, NW Himalayan foreland basin: Clues for exhumation and denudation of the Himalaya during the India-Asia collision: Geological Society of America Bulletin, v. 121, no. 3-4, p. 519–535.

Jessup, M. J., Cottle, J. M., Searle, M. P., Law, R. D., Newell, D. L., Tracy, R. J., and Waters, D. J., 2008, P–T–t–D paths of Everest Series schist, Nepal: Journal of Metamorphic Geology, v. 26, no. 7, p. 717–739.

Ji, W.-Q., Wu, F.-Y., Chung, S.-L., Li, J.-X., and Liu, C.-Z., 2009, Zircon U–Pb geochronology and Hf isotopic constraints on petrogenesis of the Gangdese batholith, southern Tibet: Chemical Geology, v. 262, no. 3-4, p. 229–245.

Jiang, S., Nie, F., Hu, P., Lai, X., and Liu, Y., 2009, Mayum: an orogenic gold deposit in Tibet, China: Ore Geology Reviews, v. 36, no. 1-3, p. 160–173.

Jiang, S., Nie, F., Hu, P., and Liu, Y., 2006, 40Ar-39Ar age, geochemical features of the Mayum adakitic porphyry in Tibet: Acta Petrologica Sinica, v. 22, no. 3.

Jiang, Z. Q., Wang, Q., Wyman, D. A., Li, Z. X., Yang, J. H., Shi, X. B., Ma, L., Tang, G. J., Gou, G. N., Jia, X. H., and Guo, H. F., 2014, Transition from oceanic to continental lithosphere subduction in southern Tibet: Evidence from the Late Cretaceous-Early Oligocene (similar to 91-30 Ma) intrusive rocks in the Chanang-Zedong area, southern Gangdese: Lithos, v. 196, p. 213-231.

Kali, E., Leloup, P. H., Arnaud, N., Mahéo, G., Liu, D., Boutonnet, E., Van der Woerd, J., Liu, X., Liu-Zeng, J., and Li, H., 2010, Exhumation history of the deepest central Himalayan rocks, Ama Drime range: Key pressure-temperature-deformation-time constraints on orogenic models: Tectonics, v. 29.

Kapp, P., Murphy, M. A., Yin, A., Harrison, T. M., Ding, L., and Guo, J., 2003, Mesozoic and Cenozoic tectonic evolution of the Shiquanhe area of western Tibet: Tectonics, v. 22, no. 4.

Kellett, D. A., Cottle, J. M., and Smit, M., 2014, Eocene deep crust at Ama Drime, Tibet: Early evolution of the Himalayan orogen: Lithosphere, v. 6, no. 4, p. 220-229.

Kellett, D. A., Grujic, D., Coutand, I., Cottle, J., and Mukul, M., 2013, The South Tibetan detachment system facilitates ultra rapid cooling of granulite-facies rocks in Sikkim Himalaya: Tectonics, v. 32, no. 2, p. 252–270.

Kellett, D. A., Grujic, D., and Erdmann, S., 2009, Miocene structural reorganization of the South Tibetan detachment, eastern Himalaya: Implications for continental collision: Lithosphere, v. 1, no. 5, p. 259-281.

Kellett, D. A., Grujic, D., Warren, C., Cottle, J., Jamieson, R., and Tenzin, T., 2010, Metamorphic history of a syn-convergent orogen-parallel detachment: The South Tibetan detachment system, Bhutan Himalaya: Journal of Metamorphic Geology, v. 28, no. 8, p. 785–808.

King, J., Harris, N., Argles, T., Parrish, R., Charlier, B., Sherlock, S., and Zhang, H. F., 2007, First field evidence of southward ductile flow of Asian crust beneath southern Tibet: Geology, v. 35, no. 8, p. 727-730.

Larson, K. P., and Cottle, J. M., 2015, Initiation of crustal shortening in the Himalaya: Terra Nova, v. 27, no. 3, p. 169-174.

Larson, K. P., Godin, L., Davis, W. J., and Davis, D. W., 2010, Out-of-sequence deformation and expansion of the Himalayan orogenic wedge: insight from the Changgo culmination, south central Tibet: Tectonics, v. 29, no. 4.

Lee, J., Hacker, B. R., Dinklage, W. S., Wang, Y., Gans, P., Calvert, A., Wan, J., Chen, W., Blythe, A. E., and McClelland, W., 2000, Evolution of the Kangmar Dome, southern Tibet: Structural, petrologic, and thermochronologic constraints: Tectonics, v. 19, no. 5, p. 872–895.

Lee, J., McClelland, W., Wang, Y., Blythe, A., and McWilliams, M., 2006, Oligocene-Miocene middle crustal flow in southern Tibet: geochronology of Mabja Dome: Geological Society, London, Special Publications, v. 268, no. 1, p. 445-469.

Lee, J., and Whitehouse, M. J., 2007, Onset of mid-crustal extensional flow in southern Tibet: Evidence from U/Pb zircon ages: Geology, v. 35, no. 1, p. 45-48.

Leloup, P. H., Liu, X., Maheo, G., Paquette, J. L., Arnaud, N., and Aubray, A., 2015, New constraints on the timing of partial melting and deformation along the Nyalam section (central Himalaya): implications for extrusion models: Geological Society, London, Special Publications, v. 412, no. 1.

Leloup, P. H., Mahéo, G., Arnaud, N., Kali, E., Boutonnet, E., Liu, D., Xiaohan, L., and Haibing, L., 2010, The South Tibet detachment shear zone in the Dinggye area Time constraints on extrusion models of the Himalayas: Earth and Planetary Science Letters, v. 292, no. 1-2, p. 1-16.

Li, C., Huang, X.-p., Mou, S.-y., and Chi, X.-g., 2006, Age dating of the Zougouyouchacuo volcanic rocks and age determination of the Kangtog Formation in southern Qiangtang, northern Tibet, China: Geological Bulletin of China, v. 25, p. 226-228.

Li, J.-X., Qin, K.-Z., Li, G.-M., Xiao, B., Chen, L., and Zhao, J.-X., 2011, Post-collisional ore-bearing adakitic porphyries from Gangdese porphyry copper belt, southern Tibet: Melting of thickened juvenile arc lower crust: Lithos, v. 126, no. 3-4, p. 265-277.

Liao, S., Chen, Z., Luo, X., and Zhou, A., 2002, Discovery of leucite phonolite in the Tangra Yumco area, Tibet, its geological significance: Geological Bulletin of China, v. 21.

Liu, D., Zhao, Z., Zhu, D.-C., Niu, Y., DePaolo, D. J., Harrison, M. T., Mo, X., Dong, G., Zhou, S., Sun, C., Zhang, Z., and Liu, J., 2014a, Postcollisional potassic and ultrapotassic rocks in southern Tibet: Mantle and crustal origins in response to India–Asia collision and convergence: Geochimica et Cosmochimica Acta, v. 143, p. 207–231.

Liu, D., Zhao, Z. D., Zhu, D. C., Niu, Y. L., and Harrison, T. M., 2014b, Zircon xenocrysts in Tibetan ultrapotassic magmas: Imaging the deep crust through time: Geology, v. 42, no. 1, p. 43-46.

Liu, X., Liu, X., Leloup, P., Maheo, G., Paquette, J., Zhang, X., and Zhou, X., 2012, Ductile deformation within Upper Himalaya Crystalline Sequence and geological implications, in Nyalam area, Southern Tibet: Chinese Science Bulletin, v. 57, no. 26, p. 3469–3481.

Mahéo, G., Guillot, S., Blichert-Toft, J., Rolland, Y., and Pêcher, A., 2002, A slab breakoff model for the Neogene thermal evolution of South Karakoram and South Tibet: Earth and Planetary Science Letters, v. 195, p. 45-58.

Maluski, H., Matte, P., Brunel, M., and Xiao, X., 1988, Argon 39-Argon 40 dating of metamorphic and plutonic events in the north and high Himalaya belts (southern Tibet-China): Tectonics, v. 7, no. 2, p. 299–326.

Martin, A., Gehrels, G., and DeCelles, P., 2007, The tectonic significance of (U,Th)/Pb ages of monazite inclusions in garnet from the Himalaya of central Nepal: Chemical Geology, v. 244, no. 1-2, p. 1-24.

Mathew, G., Sarkar, S., Pande, K., Dutta, S., Ali, S., Rai, A., and Netrawali, S., 2013, Thermal metamorphism of the Arunachal Himalaya, India: Raman thermometry and thermochronological constraints on the tectono-thermal evolution: International Journal of Earth Sciences, v. 102, no. 7, p. 1911–1936.

McCallister, A. T., Taylor, M. H., Murphy, M. A., Styron, R. H., and Stockli, D. F., 2014, Thermochronologic constraints on the late Cenozoic exhumation history of the Gurla Mandhata metamorphic core complex, Southwestern Tibet: Tectonics, v. 33, no. 2, p. 27-52.

Miller, C., Schuster, R., Klötzli, U., Frank, W., and Purtscheller, F., 1999, Post-collisional potassic and ultrapotassic magmatism in SW Tibet: Geochemical and Sr–Nd–Pb–O isotopic constraints for mantle source characteristics and petrogenesis: Journal of Petrology, v. 40, no. 9, p. 1399-1424.

Mottram, C., Warren, C., Regis, D., Roberts, N., Harris, N., Argles, T., and Parrish, R., 2014, Developing an inverted Barrovian sequence; insights from monazite petrochronology: Earth and Planetary Science Letters, v. 403, p. 418–431.

Mugnier, J.-L., and Huyghe, P., 2006, Ganges basin geometry records a pre-15 Ma isostatic rebound of Himalaya: Geology, v. 34, no. 6, p. 445-448.

Murphy, M. A., and Harrison, T. M., 1999, Relationship between leucogranites and the Qomolangma detachment in the Rongbuk Valley, south Tibet: Geology, v. 27, no. 9, p. 831-834.

Murphy, M. A., Yin, A., Kapp, P., Harrison, T. M., Manning, C. E., Ryerson, F. J., Ding, L., and Guo, J., 2002, Structural evolution of the Gurla Mandhata detachment system, southwest Tibet: Implications for the eastward extent of the Karakoram fault system: Geological Society of America Bulletin, v. 114, p. 428–447.

Najman, Y., Bickle, M., Garzanti, E., Pringle, M., Barfod, D., Brozovic, N., Burbank, D., and Ando, S., 2009, Reconstructing the exhumation history of the Lesser Himalaya, NW India, from a multitechnique provenance study of the foreland basin Siwalik Group: Tectonics, v. 28, no. 5.

Najman, Y., Garzanti, E., Pringle, M., Bickle, M., Stix, J., and Khan, I., 2003, Early-Middle Miocene paleodrainage and tectonics in the Pakistan Himalaya: Geological Society of America Bulletin, v. 115, no. 10, p. 1265-1277.

Najman, Y., Johnson, K., White, N., and Oliver, G., 2004, Evolution of the Himalayan foreland basin, NW India: Basin Research, v. 16, no. 1, p. 1–24.

Najman, Y. M. R., Pringle, M. S., Johnson, M. R. W., Robertson, A. H. F., and Wijbrans, J. R., 1997, Laser 40Ar/39Ar dating of single detrital muscovite grains from early foreland-basin sedimentary deposits in India: Implications for early Himalayan evolution: Geology, v. 25, no. 6, p. 535-538.

Nomade, S., Renne, P., Mo, X., Zhao, Z., and Zhou, S., 2004, Miocene volcanism in the Lhasa block, Tibet: spatial trends and geodynamic implications: Earth and Planetary Science Letters, v. 221, no. 1-4, p. 227–243.

Pan, F.-B., Zhang, H.-F., Harris, N., Xu, W.-C., and Guo, L., 2012, Oligocene magmatism in the eastern margin of the east Himalayan syntaxis and its implication for the India–Asia post-collisional process: Lithos, v. 154, p. 181-192.

Qu, X., Hou, Z., and Li, Z., 2003, 40Ar/39Ar ages of the ore-bearing porphyries in Gangdese copper belt and their geological significances: Acta Geologica Sinica, v. 77.

Quigley, M., Yu, L., Liu, X., Wilson, C. J. L., Sandiford, M., and Phillips, D., 2006, 40Ar/39Ar thermochronology of the Kampa Dome, southern Tibet: Implications for tectonic evolution of the North Himalayan gneiss domes: Tectonophysics, v. 421, no. 3-4, p. 269-297.

Ravikant, V., Wu, F.-Y., and Ji, W.-Q., 2009, Zircon U–Pb and Hf isotopic constraints on petrogenesis of the Cretaceous–Tertiary granites in eastern Karakoram and Ladakh, India: Lithos, v. 110, no. 1-4, p. 153-166.

Rolland, Y., Mahéo, G., Guillot, S., and Pecher, A., 2001, Tectono-metamorphic evolution of the Karakoram Metamorphic complex (Dassu-Askole area, NE Pakistan): exhumation of mid-crustal HT-MP gneisses in a convergent context: Journal of Metamorphic Geology, v. 19, p. 717–737.

Rubatto, D., Chakraborty, S., and Dasgupta, S., 2013, Timescales of crustal melting in the Higher Himalayan Crystallines (Sikkim, Eastern Himalaya) inferred from trace element-constrained monazite and zircon chronology: Contributions to Mineralogy and Petrology, v. 165, no. 2, p. 349–372.

Sachan, H., Kohn, M., Saxena, A., and Corrie, S., 2010, The Malari leucogranite, Garhwal Himalaya, northern India: Chemistry, age, and tectonic implications: Geological Society of America Bulletin, v. 122, no. 11-12, p. 1865-1876.

Schlup, M., Steck, A., Carter, A., Cosca, M., Epard, J.-L., and Hunziker, J., 2011, Exhumation history of the NW Indian Himalaya revealed by fission track and 40Ar/39Ar ages: Journal of Asian Earth Sciences, v. 40, no. 1, p. 334–350.

Schultz, M., Hodges, K. V., Van Soest, M. C., and Wartho, J. A., 2014, Thermochronologic constraints on the Miocene slip history of the South Tibetan detachment system in the Everest region, central Himalaya:
American Geophysical Union, Fall Meeting 2014, abstract #EP21A-3518.

Searle, M., Parrish, R., Hodges, K., Hurford, A., Ayres, M., and Whitehouse, M., 1997, Shisha Pangma Leucogranite, South Tibetan Himalaya: Field Relations, Geochemistry, Age, Origin, and Emplacement: The Journal of Geology, v. 105, no. 3, p. 295-318.

Searle, M. P., and Godin, L., 2003, The South Tibetan detachment and the Manaslu leucogranite: A structural reinterpretation and restoration of the Annapurna-Manaslu Himalaya, Nepal: Journal of Geology, v. 111, p. 505-523.

Searle, M. P., Noble, S. R., Hurford, A. J., and Rex, D. C., 1999, Age of crustal melting, emplacement and exhumation history of the Shivling leucogranite, Garhwal Himalaya: Geological Magazine, v. 136, no. 5, p. 513-525.

Sen, K., Chaudhury, R., and Pfänder, J., 2015, 40Ar–39Ar age constraint on deformation and brittle–ductile transition of the Main Central Thrust and the South Tibetan Detachment zone from Dhauliganga valley, Garhwal Himalaya, India: Journal of Geodynamics, v. 88, p. 1-13.

Sorcar, N., Hoppe, U., Dasgupta, S., and Chakraborty, S., 2014, High-temperature cooling histories of migmatites from the High Himalayan Crystallines in Sikkim, India: rapid cooling unrelated to exhumation?: Contributions to Mineralogy and Petrology, v. 167, no. 2.

Sorkhabi, R. B., Stump, E., Foland, K. A., and Jain, A. K., 1996, Fission-track and 40Ar/39Ar evidence for episodic denudation of the Gangotri granites in the Garhwal Higher Himalaya, India: Tectonophysics, v. 260, p. 187-199.

Spicer, R. A., Harris, N. B. W., Widdowson, M., Herman, A. B., Guo, S., Valdes, P. J., Wolfe, J. A., and Kelley, S. P., 2003, Constant elevation of southern Tibet over the past 15 million years: Nature, v. 421, no. 6923, p. 622-624.

Stearns, M. A., Hacker, B. R., Ratschbacher, L., Lee, J., Cottle, J. M., and Kylander-Clark, A., 2013, Synchronous Oligocene–Miocene metamorphism of the Pamir and the north Himalaya driven by plate-scale dynamics: Geology, v. 41, no. 10, p. 1071-1074.

Stübner, K., Grujic, D., Parrish, R. R., Roberts, N. M. W., Kronz, A., Wooden, J., and Ahmad, T., 2014, Monazite geochronology unravels the timing of crustal thickening in NW Himalaya: Lithos, v. 210-211, p. 111-128.

Sun, C., Zhao, Z., Mo, X., Zhu, D., Dong, G., Zhou, S., Dong, X., and Xie, G., 2007, Geochemistry and origin of the Miocene Sailipu ultrapotassic rocks on western Lhasa block, Tibetan Plateau: Acta Petrologica Sinica, v. 23.

Szulc, A., Najman, Y., Sinclair, H., Pringle, M., Bickle, M., Chapman, H., Garzanti, E., Andò, S., Huyghe, P., Mugnier, J. L., Ojha, T., and DeCelles, P., 2006, Tectonic evolution of the Himalaya constrained by detrital 40Ar–39Ar, Sm–Nd and petrographic data from the Siwalik foreland basin succession, SW Nepal: Basin Research, v. 18, no. 4, p. 375–391.

Thiede, R. C., Arrowsmith, J. R., Bookhagen, B., McWilliams, M. O., Sobel, E. R., and Strecker, M. R., 2005, From tectonically to erosionally controlled development of the Himalayan orogen: Geology, v. 33, no. 8, p. 689-672.

Turner, S., Arnaud, N., Liu, J., Rogers, N., Hawkesworth, C., Harris, N., Kelley, S., Van Calsteren, P., and Deng, W., 1996, Post-collision, shoshonitic volcanism on the Tibetan Plateau: implications for convective thinning of the lithosphere and the source of ocean island basalts: Journal of Petrology, v. 37, no. 1, p. 45-71.

Vance, D., Ayres, M., Kelley, S., and Harris, N., 1998, The thermal response of a metamorphic belt to extension: constraints from laser Ar data on metamorphic micas: Earth and Planetary Science Letters, v. 162, no. 1-4, p. 153–164.

Vannay, J.-C., Grasemann, B., Rahn, M., Frank, W., Carter, A., Baudraz, V., and Cosca, M., 2004, Miocene to Holocene exhumation of metamorphic crustal wedges in the NW Himalaya: Evidence for tectonic extrusion coupled to fluvial erosion: Tectonics, v. 23, no. 1.

Vannay, J. C., and Hodges, K. V., 1996, Tectonometamorphic evolution of the Himalayan metamorphic core between the Annapurna and Dhaulagiri, central Nepal: Journal of Metamorphic Geology, v. 14, p. 635–656.

Wagner, T., Lee, J., Hacker, B. R., and Seward, G., 2010, Kinematics and vorticity in Kangmar Dome, southern Tibet: Testing midcrustal channel flow models for the Himalaya: Tectonics, v. 29, no. 6.

Walker, J. D., Martin, M. W., Bowring, S. A., Searle, M. P., Waters, D. J., and Hodges, K. V., 1999, Metamorphism, melting, and extension: Age constraints from the High Himalayan Slab of southeast Zanskar and northwest Lahaul: Journal of Geology, v. 107, p. 473-495.

Wang, B., Xu, J., Chen, J., Zhang, X., Wang, L., and Xia, B., 2010, Petrogenesis and geochronology of the ore-bearing porphyritic rocks in Tangbula porphyry molybdenum-copper deposit in the eastern segment of the Gangdese metallogenic belt: Acta Petrologica Sinica, v. 26, no. 6.

Wang, J., Zhang, J., and Wang, X., 2013, Structural kinematics, metamorphic P–T profiles and zircon geochronology across the Greater Himalayan Crystalline Complex in south-central Tibet: implication for a revised channel flow: Journal of Metamorphic Geology, v. 31, no. 6, p. 607–628.

Wang, Q., Wyman, D., Xu, J., Dong, Y., Vasconcelos, P., Pearson, N., Wan, Y., Dong, H., Li, C., Yu, Y., Zhu, T., Feng, X., Zhang, Q., Zi, F., and Chu, Z., 2008, Eocene melting of subducting continental crust and early uplifting of central Tibet: Evidence from central-western Qiangtang high-K calc-alkaline andesites, dacites and rhyolites: Earth and Planetary Science Letters, v. 272, no. 1-2, p. 158–171.

Wang, Y., Li, Q., and Qu, G., 2006, 40Ar/39Ar thermochronological constraints on the cooling and exhumation history of the South Tibetan Detachment System, Nyalam area, southern Tibet: Geological Society, London, Special Publications, v. 268, no. 1, p. 327-354.

Warren, C. J., Grujic, D., Cottle, J. M., and Rogers, N. W., 2012, Constraining cooling histories: rutile and titanite chronology and diffusion modelling in NW Bhutan: Journal of Metamorphic Geology, v. 30, no. 2, p. 113–130.

Warren, C. J., Grujic, D., Kellett, D. A., Cottle, J., Jamieson, R. A., and Ghalley, K. S., 2011, Probing the depths of the India-Asia collision: U-Th-Pb monazite chronology of granulites from NW Bhutan: Tectonics, v. 30, no. 2.

Warren, C. J., Singh, A. K., Roberts, N. M. W., Regis, D., Halton, A. M., and Singh, R. B., 2014, Timing and conditions of peak metamorphism and cooling across the Zimithang Thrust, Arunachal Pradesh, India: Lithos, v. 200, p. 94-110.

Webb, A., Schmitt, A., He, D., and Weigand, E., 2011a, Structural and geochronological evidence for the leading edge of the Greater Himalayan Crystalline complex in the central Nepal Himalaya: Earth and Planetary Science Letters, v. 304, no. 3-4, p. 483–495.

Webb, A. A. G., Yin, A., Harrison, T. M., Célérier, J., Gehrels, G. E., Manning, C. E., and Grove, M., 2011b, Cenozoic tectonic history of the Himachal Himalaya (northwestern India) and its constraints on the formation mechanism of the Himalayan orogen: Geosphere, v. 7, no. 4, p. 1013-1061.

White, N., Pringle, M., Garzanti, E., Bickle, M., Najman, Y., Chapman, H., and Friend, P., 2002, Constraints on the exhumation and erosion of the High Himalayan Slab, NW India, from foreland basin deposits: Earth and Planetary Science Letters, v. 195, no. 1-2, p. 29-44.

Williams, H., Turner, S., Kelley, S., and Harris, N., 2001, Age and composition of dikes in Southern Tibet: New constraints on the timing of east-west extension and its relationship to postcollisional volcanism: Geology, v. 29, no. 4, p. 339-342.

Williams, H. M., Turner, S. P., Pearce, J. A., Kelley, S. P., and Harris, N. B. W., 2004, Nature of the Source Regions for Post-collisional, Potassic Magmatism in Southern and Northern

Tibet from Geochemical Variations and Inverse Trace Element Modelling: Journal of Petrology, v. 45, no. 3.

Wu, C., Nelson, K. D., Wortman, G., Samson, S. D., Yue, Y., Li, J., Kidd, W. S. F., and Edwards, M. A., 1998, Yadong cross structure and South Tibetan Detachment in the east central Himalaya (89°-90°E): Tectonics, v. 17, no. 1, p. 28-45.

Xu, W.-C., Zhang, H.-F., Guo, L., and Yuan, H.-L., 2010a, Miocene high Sr/Y magmatism, south Tibet: Product of partial melting of subducted Indian continental crust and its tectonic implication: Lithos, v. 114, no. 3-4, p. 293-306.

Xu, W.-C., Zhang, H.-F., Parrish, R., Harris, N., Guo, L., and Yuan, H.-L., 2010b, Timing of granulite-facies metamorphism in the eastern Himalayan syntaxis and its tectonic implications: Tectonophysics, v. 485, no. 1-4, p. 231-244.

Xu, Z., Wang, Q., Pêcher, A., Liang, F., Qi, X., Cai, Z., Li, H., Zeng, L., and Cao, H., 2013, Orogen-parallel ductile extension and extrusion of the Greater Himalaya in the late Oligocene and Miocene: Tectonics, v. 32, no. 2, p. 191-215.

Yan, D.-P., Zhou, M.-F., Robinson, P., Grujic, D., Malpas, J., Kennedy, A., and Reynolds, P., 2012, Constraining the mid-crustal channel flow beneath the Tibetan Plateau: data from the Nielaxiongbo gneiss dome, SE Tibet: International Geology Review, v. 54, no. 6, p. 615-632.

Yin, A., Harrison, T. M., Ryerson, F. J., Chen, W., Kidd, W. S. F., and Copeland, P., 1994, Tertiary structural evolution of the Gangdese thrust system, southeastern Tibet: Journal of Geophysical Research, v. 99, no. B9, p. 18175–18201.

Zeiger, K., Gordon, S., Long, S., Kylander-Clark, A., Agustsson, K., and Penfold, M., 2015, Timing and conditions of metamorphism and melt crystallization in Greater Himalayan rocks, eastern and central Bhutan: insight from U–Pb zircon and monazite geochronology and trace-element analyses: Contributions to Mineralogy and Petrology, v. 169, no. 5.

Zhang, H., Harris, N., Guo, L., and Xu, W., 2010, The significance of Cenozoic magmatism from the western margin of the eastern syntaxis, southeast Tibet: Contributions to Mineralogy and Petrology, v. 160, no. 1.

Zhang, H., Harris, N., Parrish, R., Kelley, S., Zhang, L., Rogers, N., Argles, T., and King, J., 2004, Causes and consequences of protracted melting of the mid-crust exposed in the North Himalayan antiform: Earth and Planetary Science Letters, v. 228, no. 1-2, p. 195–212.

Zhang, J., and Guo, L., 2007, Structure and geochronology of the southern Xainza-Dinggye rift and its relationship to the south Tibetan detachment system: Journal of Asian Earth Sciences, v. 29, no. 5-6, p. 722–736.

Zhang, J., Santosh, M., Wang, X., Guo, L., Yang, X., and Zhang, B., 2012, Tectonics of the northern Himalaya since the India–Asia collision: Gondwana Research, v. 21, no. 4, p. 939–960.

Zhang, L.-Y., Ducea, M. N., Ding, L., Pullen, A., Kapp, P., and Hoffman, D., 2014, Southern Tibetan Oligocene–Miocene adakites: A record of Indian slab tearing: Lithos, v. 210, p. 209-223.

Zhao, Z., Mo, X., Dilek, Y., Niu, Y., DePaolo, D. J., Robinson, P., Zhu, D., Sun, C., Dong, G., and Zhou, S., 2009, Geochemical and Sr–Nd–Pb–O isotopic compositions of the post-collisional ultrapotassic magmatism in SW Tibet: Petrogenesis and implications for India intra-continental subduction beneath southern Tibet: Lithos, v. 113, no. 1-2, p. 190-212.

Zhao, Z., Mo, X., Nomade, S., Renne, P. R., Zhou, S., Dong, G., Wang, L., Zhu, D., and Liao, Z., 2006, Post-collisional ultrapotassic rocks in Lhasa Block, Tibetan Plateau: Spatial and temporal distribution and its' implications: Acta Petrologica Sinica, v. 22, no. 4.

Zheng, Y.-C., Hou, Z.-Q., Li, Q.-Y., Sun, Q.-Z., Liang, W., Fu, Q., Li, W., and Huang, K.-X., 2012a, Origin of Late Oligocene adakitic intrusives in the southeastern Lhasa terrane: Evidence from in situ zircon U–Pb dating, Hf–O isotopes, and whole-rock geochemistry: Lithos, v. 148, p. 296-311.

Zheng, Y.-C., Hou, Z.-Q., Li, W., Liang, W., Huang, K.-X., Li, Q.-Y., Sun, Q.-Z., Fu, Q., and Zhang, S., 2012b, Petrogenesis and Geological Implications of the Oligocene Chongmuda-Mingze Adakite-Like Intrusions and Their Mafic Enclaves, Southern Tibet: The Journal of Geology, v. 120, no. 6, p. 647-669.

Zheng, Y., Zhang, G., Xu, R., Gao, S., Pang, Y., Cao, L., Du, A., and Shi, Y., 2007, Geochronologic constraints on magmatic intrusions and mineralization of the Zhunuo porphyry copper deposit in Gangdese, Tibet: Chinese Science Bulletin, v. 52, no. 22.

Zhou, S., 2002, Study on the geochronology of pivotal regions of Gangdese magmatic, Yarlung Zangbo ophiolite belts, Tibet: China U. Geosciences, Beijing.

Zhou, S., Mo, X., Zhao, Z., Qiu, R., Niu, Y., Guo, T., and Zhang, S., 2010, 40Ar/39Ar geochronology of post-collisional volcanism in the middle Gangdese Belt, southern Tibet: Journal of Asian Earth Sciences, v. 37, no. 3, p. 246–258.